PHYSICS AND CHEMISTRY OF SOLID STATE
V. 26, No.1 (2025) pp. 124-131
Section: Chemistry

DOI: 10.15330/pcss.26.1.124-131

Vasyl Stefanyk Precarpathian National University

ФІЗИКА І ХІМІЯ ТВЕРДОГО ТІЛА
Т. 26, № 1 (2025) С. 124-131
Хімічні науки

PACS: 68.43.-h

ISSN 1729-4428 (Print)
ISSN 2309-8589 (Online)

Iryna Starko

Purification of polluted water with La- and Gd-doped spinel ferrite nanoparticles: adsorption kinetics and mechanisms

Vasyl Stefanyk Precarpathian National University, Ivano-Frankivsk, Ukraine, starkoiryna93@gmail.com

In this work, the removal of the CR dye and OTC antibiotic from aqueous solutions by as-prepared and annealed La- and Gd-substituted nanoferrites was investigated. The kinetic models of PFO, PSO, Elovich, and IPD were used to evaluate the adsorption mechanism. It was shown, that the adsorption of CR and OTC on the ferrites is the best fitted with the pseudo-second-order kinetic model. The adsorption equilibrium towards the CR and OTC was reached at 60 minutes for both pollutants. The annealing impacts the samples' adsorption properties, increasing the initial rate of adsorption as per the PSO kinetic model. In particular, the initial rate of the CR adsorption on the as-synthesized and annealed La- and Gd-containing ferrites is increased approximately 7 and 5 times, respectively. The rate of OTC adsorption also increased in the samples after annealing. For the $Ni_{0.5}Co_{0.5}La_{0.02}Fe_{1.98}O_4$ sample, the rate improved by 1.8 times. In the case of the $Ni_{0.5}Co_{0.5}Gd_{0.025}Fe_{1.975}O_4$ sample, the rate increased by 3.6 times. The analyzed data shows that the dye and antibiotic molecules are adsorbed on the ferrite's surface through a chemisorption.

Keywords: Ni-Co ferrite; lanthanum; gadolinium; adsorbent; kinetics model; spinel; water treatment.

Received 12 October 2025; Accepted 25 February 2025.

Introduction

Magnetic nanomaterials have found a wide range of applications [1–3]. For example, they can be used as adsorbents in water purification from dyes and antibiotics [4–6]. The main physicochemical interactions that are responsible for the removal of various pollutants from wastewater by adsorption are chemisorption, physisorption, ion exchange, hydrophobic interaction, electrostatic attraction, weak Van der Waals forces, hydrogen bonding, complexation, dipole-dipole interaction, π-π interaction, etc. [5,7,8]. The adsorption mechanisms depend on the type of pollutant and type of ferrite adsorbent. The adsorption properties of $CoFe_2O_4$ synthesized by the hydrothermal method were studied in [9] and the mechanism of Congo Red adsorption by the nanoferrite surface was described. In this study, it was proved that CR adsorption is positively affected by the increase in the surface charge of the adsorbent, and the mechanism of adsorption of anionic dye on the surface of $CoFe_2O_4$ is explained based on the principle of electrostatic attraction. The adsorption mechanism of Congo Red by the surface of $CoFe_2O_4$ and $NiFe_2O_4$, synthesized by the hydrothermal method, and studied in the work [10], is also electrostatic attraction and chemisorption, which was proven based on adsorption kinetics, thermodynamics, and the experimental data. The chemisorption of Congo Red dye by the surface of $CoFe_2O_4$ and $NiFe_2O_4$, synthesized by the sol-gel method, was described according to the Dubinin-Radushkevich model in work [11]. Also, the chemisorption of CR dye by the $Co_{0.5}Mn_{0.5}Fe_2O_4$ nanoferrite was confirmed in the study [4] based on the kinetic data and pseudo-second-order kinetic model.

Literature analysis shows that the main mechanisms of antibiotic adsorption are chemisorption, H-bonding, and electrostatic attraction. For example, the adsorption mechanism of the tetracycline removal by the $CoFe_2O_4$ and $NiFe_2O_4$, synthesized by the coprecipitation method, is not only electrostatic attraction but also chemisorption, which occurs due to H-bonding between the surface hydroxyl groups of nanoferrites and the C=O group of the

tetracycline molecule [12]. The chemisorption of the antibiotic oxytetracycline (OTC) on the surface of the $NiFe_2O_4$/Au composite is described based on a pseudo-second-order kinetic model and presented in the study [13].

The structure and physicochemical properties of spinel ferrites can be significantly modified by doping/substituting with divalent or trivalent metals. In this regard, the replacement of Fe^{3+} ions with rare earth elements (REEs) is widely known for its ability to improve the structure, morphology, and other physicochemical characteristics of spinel ferrites [14]. REEs include 17 heavy metals: 15 elements of the lanthanide group, as well as Scandium and Yttrium, which have the same chemical properties [15]. REEs have a larger ionic radius compared to the iron atom, which indicates that the atoms easily fit into the octahedral sites of the spinel structure. Therefore, currently, in the field of spinel ferrite research, the use of REEs for the synthesis of nanomaterials is increasing. However, there are very little amount of the papers related to the adsorption properties of REE-substituted spinel ferrites.

The aim of this work is to perform the adsorption kinetic studies on Congo Red dye and oxytetracycline antibiotic removal by the $Ni_{0.5}Co_{0.5}La_{0.02}Fe_{1.98}O_4$ and $Ni_{0.5}Co_{0.5}Gd_{0.025}Fe_{1.975}O_4$ ferrites. The effect of the thermal treatment of the sample on the adsorption rate will be studied.

I. Experimental

1.1. Materials and methods.

Nanoferrite corresponding to $Ni_{0.5}Co_{0.5}Re_xFe_{2-x}O_4$ (Re=La or Gd) composition was synthesized by the reductive method using sodium borohydride (reducing agent and precipitant). The detailed synthesis methodology was presented in the study [16]. In brief, stoichiometric amounts of nickel(II) nitrate, cobalt(II) acetate, iron(III) nitrate, and lanthanum nitrate (or gadolinium nitrate) were dissolved in distilled water. Then 0.4M $NaBH_4$ solution was slowly added to the metal salt solution under constant stirring at 50°C. The resulting mixture was heated to 70°C for 2.5 hours. After that, the mixture was left for 15 hours and then heated to 70°C for 3 hours. The resulting powder was washed with a large amount of distilled water and dried. After that, the part of the obtained powder was annealed at 600°C for 4 hours. This choice of temperature was confirmed by thermogravimetric analysis [16] and promotes the formation of the spinel structure while preserving the active surface.

1.2. Adsorption experiments

The adsorption kinetic studies were carried out using 60 mg of adsorbents and 150 mL of the corresponding pollutant (CR or OTC) with an initial concentration of 10 mg/L. The adsorbent was introduced into the pollutant solution and mixed using an overhead mixer. During the adsorption process, aliquots of the pollutant solutions were taken at certain intervals, and the sorbent residues were collected using a neodymium magnet. The concentration of the dye or antibiotic was analyzed using a ULAB 102-UV spectrophotometer by monitoring the absorption at a wavelength of 500 or 356 nm, respectively. The adsorption capacity was determined according to the equation (1) [17]:

$$q_t = \frac{(C_0 - C_t)\cdot V}{m}, \quad (1)$$

where q_t is the adsorption capacity (mg/g), C_0 is the initial CR or OTC concentration, C_t is CR or OTC concentration at time t, V is the volume of the solution (L), and m is the mass of the spinel ferrites (g). The nonlinear kinetic models were applied to fit the data.

II. Results and discussion

2.1. Adsorption studies towards Congo red dye removal

Fig.1 shows the dependence of the amount of adsorbed anionic dye q_t (mg/g) versus the contact time t (min) onto as-synthesized (Fig.1a,b) and annealed (Fig.1c,d) $Ni_{0.5}Co_{0.5}La_{0.02}Fe_{1.98}O_4$ adsorbents surface. We observe a gradual increase in the adsorption capacity of $Ni_{0.5}Co_{0.5}La_{0.02}Fe_{1.98}O_4$ nanoferrite versus time for both samples. The initial rate of adsorption is higher for the annealed sample compared to as-synthesized (Figs.1a and 1c). This can be explained by the fact that on the surface of La doped Ni-Co ferrite, the adsorption site was occupied, and other functional groups on the surface of $Ni_{0.5}Co_{0.5}La_{0.02}Fe_{1.98}O_4$ were reduced [4]. Figs.1b,d shows a comparison of the spectra before and after adsorption of Congo Red dye ($[CR]_0$ = 10 mg/L), as well as a photo illustrating the magnetic properties before and after adsorption for synthesized (Fig.1b) and annealed (Fig.1d) samples with the composition of $Ni_{0.5}Co_{0.5}La_{0.02}Fe_{1.98}O_4$.

To study the adsorption mechanism, the adsorption kinetics data were analyzed using nonlinear equations and the OriginPro 2018 software using the following adsorption models: pseudo-first-order kinetics model (PFO), pseudo-second-order kinetics model (PSO), Elovitch model, and intraparticle diffusion (IPD) model. The corresponding equations are summarized in Table 1 (equations (2)–(5)) [18,19]. The pseudo-first-order kinetics model assumes that the adsorption mechanism on the adsorbent surface will be physical sorption, while the pseudo-second-order kinetics model indicates that the adsorption process is chemisorption [4]. The Elovich model complements the pseudo-second-order kinetics model, indicating that the adsorbent surface is heterogeneous [20]. The intraparticle diffusion model indicates that the adsorption mechanism is described by the transfer of the adsorbate from the solution to the solid phase, and the adsorption rate is controlled by internal diffusion [5].

Thus, the experimental data were fitted by the adsorption kinetics models and the obtained parameters are presented in Table 2. From the obtained kinetic model parameters, we observe that the PSO kinetic model agrees well with experimental data. This is evidenced by the higher values of the correlation coefficient R^2 and the lower values of χ^2: R^2= 0.989 and χ^2= 0.48 for the as-synthesized sample, and R^2=0.944, χ^2= 0.53 for the annealed ones.

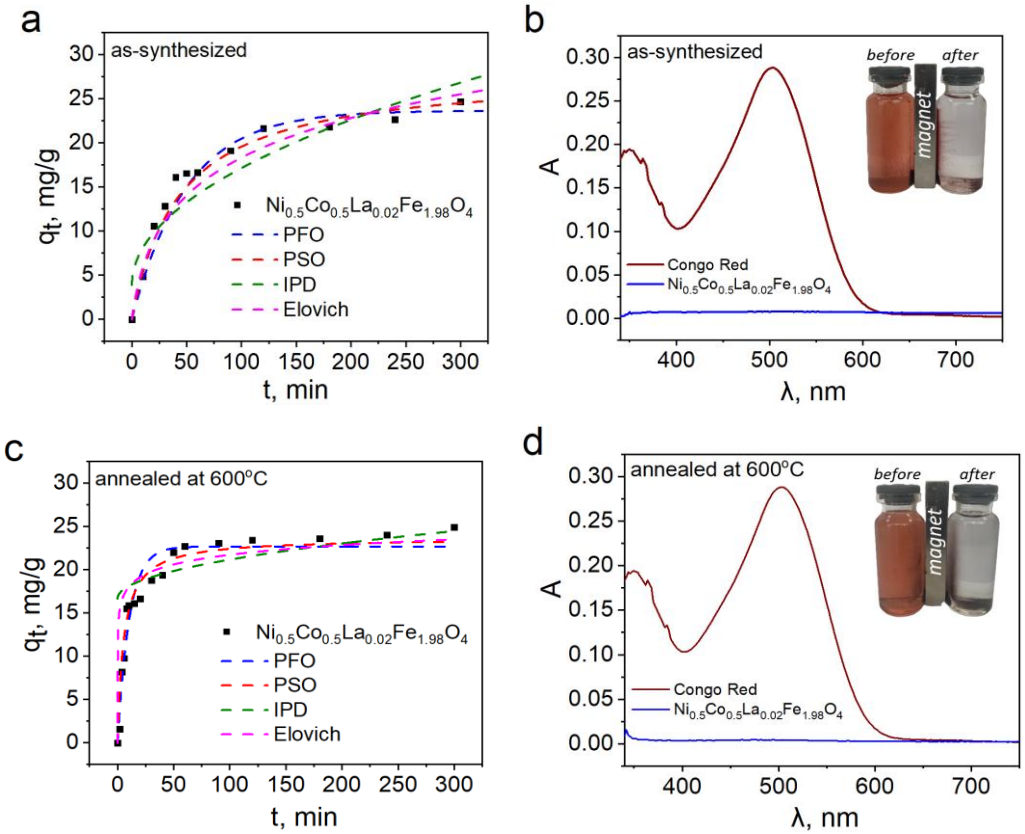

Fig. 1. Congo Red dye adsorption data and kinetic models: pseudo-first-order kinetics model (PFO), pseudo-second-order kinetics model (PSO), intraparticle diffusion model (IPD), Elovich model for Congo Red adsorption onto (a) as-synthesized and (c) annealed La-doped ferrites. Spectra of the CR dye before and after the adsorption experiment onto (b) as-synthesized and (d) annealed sample (inset photos illustrate the magnetic properties of ferrite ($[CR]_0$ = 10 mg/L).

Table 1.

Kinetic models and their equations for adsorption kinetics.

Model	Equation
Pseudo-first-order kinetics model	$q_t = (q_e - e^{-k_1 t})$ (2)
Pseudo-second-order kinetics model	$q_t = \frac{k_2 q_e^2 t}{1+k_2 q_e t}$ (3)
Elovich model	$q_t = \frac{1}{\beta}\ln(1+\alpha\beta t)$ (4)
Intraparticle diffusion model	$q_t = k_{IPD} t^{1/2} + C$ (5)
q_t (mg/g) is adsorption over time, q_e (mg/g) - adsorption at equilibrium, k_{IPD} (mg/g $min^{1/2}$) - the intraparticle diffusion rate constant, C (mg/g) - the boundary layer thickness, k_1(min^{-1}) is the PFO rate constant, k_2 (g/mg min) is the PSO rate constant, $k_2q^2_e$ or h (mg/g min) is the initial PSO adsorption rate, α (mg/g min) is the Elovich initial adsorption rate, β (g/mg) - desorption constant.	

The adsorption capacity (23.64 mg/g) calculated according to the PSO model equation is close to the experimental value (24.91 mg/g) for the annealed sample. It should be noted that the initial adsorption rate h and the constant rate k_2 are increased after the sample sintering. They equal h=4.303 mg·g^{-1}·min^{-1} and k_2=0.0077 g·mg^{-1}·min^{-1} for annealed sample h=0.629 mg·g^{-1}·min^{-1}, k_2=0.0008 g·mg^{-1}·min^{-1} compared to the as-synthesized sample. It is observed that adsorption equilibrium is reached faster for the annealed sample (in 60 min), compared to the as-synthesized sample (180 min). The Elovich model and the intraparticle diffusion model had relatively lower correlation coefficient values (Table 2), so they were not used to describe the adsorption mechanism. Therefore, the obtained results indicate that the adsorption mechanism of the CR dye on the $Ni_{0.5}Co_{0.5}La_{0.02}Fe_{1.98}O_4$ surface was chemisorption.

Fig. 2 demonstrates the adsorption of CR dye on the surface of as-synthesized and annealed Gd-containing Ni-Co ferrites and the fitting of experimental data by the same kinetics models as the above-mentioned. The parameters, presented in Table 2, show that the PSO model best fits the experimental data compared to the other kinetic models. The correlation coefficient is 0.994 and 0.961 for the as-synthesized and annealed $Ni_{0.5}Co_{0.5}Gd_{0.025}Fe_{1.975}O_4$ samples, and the χ^2 value is close to 0. The h and k_2 constants are higher for the annealed Gd-containing sample, and for this sample, the adsorption equilibrium is reached faster. This is also observed in the kinetic curves: for the as-synthesized sample, the adsorption equilibrium

Table 2.

Parameters of the kinetics model of Congo Red onto ferrites

Model	Parameter	$Ni_{0.5}Co_{0.5}La_{0.02}Fe_{1.98}O_4$ as-synthesized	$Ni_{0.5}Co_{0.5}La_{0.02}Fe_{1.98}O_4$ annealed at 600ºC	$Ni_{0.5}Co_{0.5}Gd_{0.025}Fe_{1.975}O_4$ as-synthesized	$Ni_{0.5}Co_{0.5}Gd_{0.025}Fe_{1.975}O_4$ annealed at 600ºC
	$q_{e,exp}$	24.65	24.91	24.21	24.38
PFO	k_1	0.020	0.095	0.015	0.051
	$q_{1,e}$	23.64	22.67	23.32	22.49
	R^2	0.927	0.944	0.956	0.925
	χ^2	1.78	3.57	2.63	4.38
PSO	k_2	0.0008	0.0077	0.0005	0.0035
	$q_{2,e}$	28.04	23.64	29.24	24.18
	h	0.629	4.303	0.427	2.046
	R^2	0.989	0.944	0.994	0.961
	χ^2	0.48	0.53	0.212	0.62
IPD	K_{IPD}	1.323	0.449	1.389	0.706
	C	3.904	16.671	2.051	12.876
	R^2	0.860	0.359	0.919	0.536
Elovich	α	0.929	11.197	0.612	8.594
	β	0.146	0.619	0.129	0.390
	R^2	0.962	0.638	0.976	0.887
	χ^2	1.49	0.69	0.97	1.18

is reached after 180 min, whereas for the annealed sample – after 60 min. Since the adsorption rate is proportional to the square of the dye concentration, in this case, the CR on the surface of $Ni_{0.5}Co_{0.5}Gd_{0.025}Fe_{1.975}O_4$, the adsorption process is controlled by chemisorption between the molecules of the CR and Gd-containing Ni-Co ferrites, as was observed in the case of La-containing Ni-Co ferrites. The Elovich model (Table 2) is used to study chemisorption processes and is typical for adsorbents with heterogeneous surfaces [18]. The fitting by the Elovich model shows that the as-synthesized $Ni_{0.5}Co_{0.5}Gd_{0.025}Fe_{1.975}O_4$ sample demonstrates the highest correlation coefficient value (R^2=0.976) and this value decreases to R^2=0.887 for the annealed Gd-containing Ni-Co ferrites. The successful fitting by the Elovich model is also evidenced by the low χ^2 values, which are 0.97 and 1.18 for as-synthesized and annealed ferrites. The adsorption rate parameter α is larger for the annealed $Ni_{0.5}Co_{0.5}Gd_{0.025}Fe_{1.975}O_4$ sample and is consistent with the data of the pseudo-second-order kinetic model. The desorption coefficient β is low and equals 0.129 and 0.390 for the as-synthesized and annealed samples, respectively, indicating a high adsorption capacity of Gd-containing ferrites. Therefore, the adsorption process of Congo Red dye on the $Ni_{0.5}Co_{0.5}Gd_{0.025}Fe_{1.975}O_4$ surface is chemisorption. Fig.2b,d shows a comparison of the spectra before and after CR adsorption ($[CR]_0$ = 10 mg/L), as well as a photo illustrating the magnetic properties before and after adsorption for as-synthesized (Fig.2b) and annealed (Fig.2d) samples with the composition of $Ni_{0.5}Co_{0.5}Gd_{0.025}Fe_{1.975}O_4$.

2.2. Adsorption studies towards oxytetracycline removal.

The adsorption of the oxytetracycline antibiotic was investigated on La- and Gd-doped Ni-Co ferrites at 293 K ($[OTC]_0$ = 10 mg/L). For this purpose, curves of the adsorbed antibiotic molecule (q_t) versus time (t) were constructed for synthesized and annealed La- and Gd-containing ferrites, which are presented in Fig.3. The PFO, PSO, Elovich, and IPD models were also used to explain the adsorption mechanism, and the results of the nonlinear model approximation are listed in Table 3. The fitting of the experimental data with the theoretical kinetics models can be seen in Fig. 3.

To determine the best model, the values of R^2 and χ^2 have been taken into account. After analyzing the data, it was concluded that the OTC adsorption onto $Ni_{0.5}Co_{0.5}La_{0.02}Fe_{1.98}O_4$ and $Ni_{0.5}Co_{0.5}Gd_{0.025}Fe_{1.975}O_4$ ferrites is best described by a PSO kinetic model, as evidenced by the low values of χ^2 and high values of R^2. The experimental adsorption capacity for La-containing ferrites is 20.95 (for as-synthesized) and 18.26 mg/g (for annealed), whereas the values calculated according to the PSO model are 22.43 and 20.47 mg/g, respectively.

For Gd-containing ferrites, $q_e \approx 20$ mg/g for both samples and the calculated value is 21.09 (for the as-synthesized sample) and 22.11 mg/g (for the annealed sample). Therefore, it can be concluded that the adsorption process between magnetic adsorbents and the

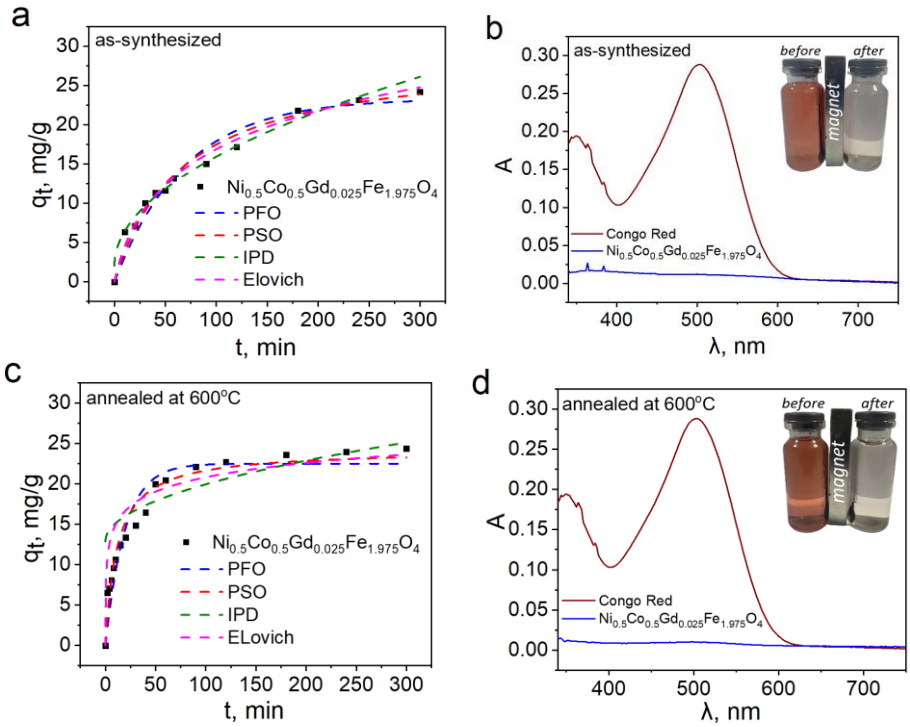

Fig. 2. Congo Red dye adsorption data and kinetic models: pseudo-first-order kinetics model (PFO), pseudo-second-order kinetics model (PSO), intraparticle diffusion model (IPD), Elovich model for Congo Red adsorption onto (a) as-synthesized and (c) annealed Gd-doped ferrites. Spectra of the CR dye before and after the adsorption experiment onto (b) as-synthesized and (d) annealed sample (inset photos illustrate the magnetic properties of ferrite ($[CR]_0$ = 10 mg/L).

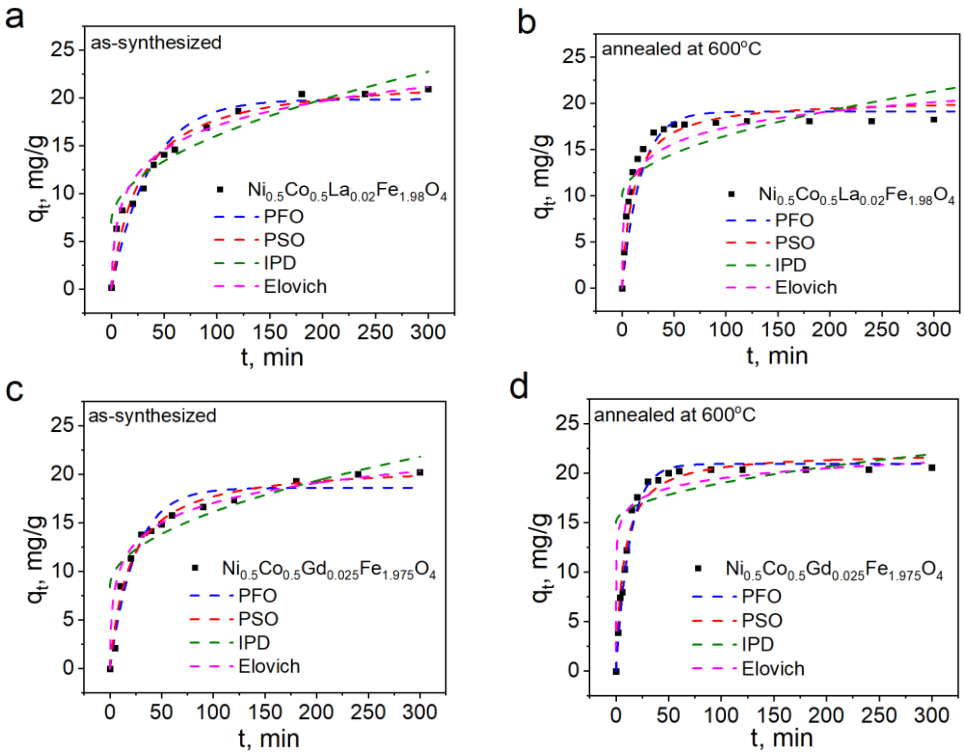

Fig. 3. Oxytetracycline adsorption data and kinetic models: pseudo-first-order kinetics model (PFO), pseudo-second-order kinetics model (PSO), intraparticle diffusion model (IPD), Elovich model for oxytetracycline adsorption onto (a,b) La- and (c,d) Gd-doped ferrites.

Table 3.

Parameters of the kinetics models for the oxytetracycline adsorption onto ferrites surface.

Model	Parameter	$Ni_{0.5}Co_{0.5}La_{0.02}Fe_{1.98}O_4$ as-synthesized	$Ni_{0.5}Co_{0.5}La_{0.02}Fe_{1.98}O_4$ annealed at 600°C	$Ni_{0.5}Co_{0.5}Gd_{0.025}Fe_{1.975}O_4$ as-synthesized	$Ni_{0.5}Co_{0.5}Gd_{0.025}Fe_{1.975}O_4$ annealed at 600°C
	$q_{e,exp}$	20.95	18.26	20.21	20.57
PFO	k_1	0.028	0.056	0.04069	0.077
	$q_{1,e}$	19.85	19.11	18.61	20.93
	R^2	0.929	0.698	0.955	0.941
	χ^2	3.08	2.29	1.87	0.51
PSO	k_2	0.002	0.005	0.003	0.006
	$q_{2,e}$	22.43	20.47	21.09	22.11
	h	1.006	1.886	1.111	3.943
	R^2	0.961	0.992	0.979	0.977
	χ^2	1.56	0.78	0.88	1.11
IPD	K_{IPD}	0.911	0.656	0.774	0.401
	C	6.964	9.928	8.391	14.986
	R^2	0.744	0.558	0.785	0.357
Elovich	α	3.680	26.68	9.229	12.344
	β	0.269	0.402	0.33	0.693
	R^2	0.922	0.895	0.907	0.835
	χ^2	1.35	1.02	1.17	0.55

OTC antibiotic molecule was a chemisorption. It should be noted that for annealed La- and Gd-substituted ferrites, adsorption equilibrium is reached faster, namely after 50 min ($Ni_{0.5}Co_{0.5}La_{0.02}Fe_{1.98}O_4$) and 60 min ($Ni_{0.5}Co_{0.5}Gd_{0.025}Fe_{1.975}O_4$), while for synthesized samples it is 180 and 240 min for La- and Gd-substituted ferrites, respectively. This can be confirmed based on the initial h and constant k_2 rate constants. From Table 3, it can be seen that the constant rate is 2 times higher for annealed La- and Gd-substituted ferrites and the initial rate is 1.8 times higher for $Ni_{0.5}Co_{0.5}La_{0.02}Fe_{1.98}O_4$ sample and 3.6 times higher for $Ni_{0.5}Co_{0.5}Gd_{0.025}Fe_{1.975}O_4$ sample. It follows that the initial rate for Gd-containing ferrites is 2 times higher than for La-substituted ferrites. This can be explained by the difference in radii of Gd and La ions, which will affect the structure of ferrite and change its surface energy (r(Gd) < r(La)). This may contribute to faster attachment of OTC antibiotic molecules on the surface of Gd-containing ferrites.

2.3. Adsorption mechanisms.

Based on the analysis of kinetic models, it is possible to schematically depict the chemisorption mechanism of Congo Red dye and oxytetracycline adsorption on the studied nanoferrites with the composition $Ni_{0.5}Co_{0.5}Re_xFe_{2-x}O_4$ (Re=La or Gd), which is presented in Fig. 4. It can be assumed that chemisorption, first of all, occurred due to H-bonds between OH_2^+ of the ferrite surface and H^+ from the NH_2-group of the CR dye, or H^+ of the phenyl or amino group of the OTC antibiotic [21].

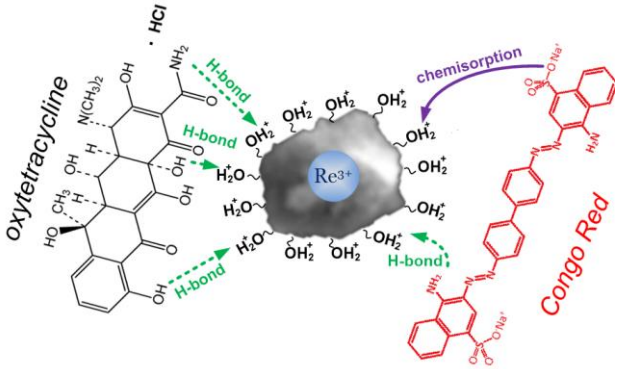

Fig. 4. The mechanism of CR and OTC adsorption on the $Ni_{0.5}Co_{0.5}Re_xFe_{2-x}O_4$ (Re=La or Gd) surface.

Conclusions

This study demonstrates the applicability of $Ni_{0.5}Co_{0.5}Re_xFe_{2-x}O_4$ (Re=La or Gd) samples as adsorbents for the removal of Congo Red dye and oxytetracycline antibiotics from water. The adsorption mechanism of CR and OTC was studied using pseudo-first-order, pseudo-second-order, Elovich, and intraparticle model kinetics models. For all studied La- and Gd-containing Ni-Co ferrites, the adsorption process was best described by a pseudo-second-order kinetic model. This is evidenced by high correlation coefficients R^2 and low χ^2 values. Therefore, the adsorption mechanism of the dye and antibiotic is explained by chemisorption. The results showed that the adsorption process is affected by the

thermal treatment of ferrites, namely their annealing at 600°C. Annealed ferrites remove CR three times faster than synthesized samples. For OTC removal, La-doped ferrites reach equilibrium 3.6 times faster, and Gd-containing Ni-Co ferrites are 4 times faster compared to as-synthesized ferrites.

Starko Iryna – PhD student.

[1] T. Tatarchuk, *Studying the Defects in Spinel Compounds: Discovery, Formation Mechanisms, Classification, and Influence on Catalytic Properties*, Nanomaterials, 14 (2024); https://doi.org/10.3390/nano14201640.
[2] K. Cai, W. Shen, B. Ren, J. He, S. Wu, W. Wang, *A phytic acid modified $CoFe_2O_4$ magnetic adsorbent with controllable morphology, excellent selective adsorption for dyes and ultrastrong adsorption ability for metal ions*, Chem. Eng. J., 330, 936 (2017); https://doi.org/10.1016/j.cej.2017.08.009.
[3] T. Tatarchuk, A. Shyichuk, V. Kotsyubynsky, N. Danyliuk, *Catalytically active cobalt ferrites synthesized using plant extracts: Insights into structural, optical, and catalytic properties*, Ceramics International, 51, 4988 (2025); https://doi.org/https://doi.org/10.1016/j.ceramint.2024.11.470.
[4] X. Zhang, Y. Xia, Z. Wang, *Adsorption of Congo red on magnetic cobalt-manganese ferrite nanoparticles: Adsorption kinetic, isotherm, thermodynamics, and electrochemistry*, PloS One, 19, e0307055 (2024); https://doi.org/10.1371/journal.pone.0307055.
[5] D.H.K. Reddy, Y.S. Yun, *Spinel ferrite magnetic adsorbents: Alternative future materials for water purification*?, Coordination Chemistry Reviews, 315, 90 (2016); https://doi.org/10.1016/j.ccr.2016.01.012.
[6] R. Sivashankar, A.B. Sathya, K. Vasantharaj, V. Sivasubramanian, *Magnetic composite an environmental super adsorbent for dye sequestration – A review*, Environmental Nanotechnology, Monitoring & Management, 1–2, 36 (2014); https://doi.org/https://doi.org/10.1016/j.enmm.2014.06.001.
[7] K.K. Kefeni, B.B. Mamba, T.A.M. Msagati, *Application of spinel ferrite nanoparticles in water and wastewater treatment: A review*, Separation and Purification Technology, 188, 399 (2017); https://doi.org/10.1016/j.seppur.2017.07.015.
[8] T. Tatarchuk, L. Soltys, W. Macyk, *Magnetic adsorbents for removal of pharmaceuticals: A review of adsorption properties*, Journal of Molecular Liquids, 384, 122174 (2023); https://doi.org/10.1016/j.molliq.2023.122174.
[9] L. Zhang, J. Lian, L. Wang, J. Jiang, Z. Duan, L. Zhao, *Markedly enhanced coercive field and Congo red adsorption capability of cobalt ferrite induced by the doping of non-magnetic metal ions*, Chemical Engineering Journal, 241, 384 (2014); https://doi.org/10.1016/j.cej.2013.10.071.
[10] L. Wang, J. Li, Y. Wang, L. Zhao, Q. Jiang, *Adsorption capability for Congo red on nanocrystalline MFe_2O_4 (M=Mn, Fe, Co, Ni) spinel ferrites*, Chemical Engineering Journal. 181–182, 72 (2012); https://doi.org/10.1016/j.cej.2011.10.088.
[11] P. Samoila, C. Cojocaru, I. Cretescu, C.D. Stan, V. Nica, L. Sacarescu, V. Harabagiu, *Nanosized spinel ferrites synthesized by sol-gel autocombustion for optimized removal of azo dye from aqueous solution*, Journal of Nanomaterials, (2015); https://doi.org/10.1155/2015/713802.
[12] J.Y.D. Alessandro Idehara, D.A. Fagundes, L.V. Leonel, L.E. Fernandez-Outon, R. de Mendonça, A.S. Albuquerque, J.D. Ardisson, *Investigation of the adsorption of the tetracycline antibiotic by $NiFe_2O_4$ and $CoFe_2O_4$ nanoparticles*, Environmental Nanotechnology, Monitoring and Management, 20, 100830 (2023); https://doi.org/10.1016/j.enmm.2023.100830.
[13] T.P. Nguyen, Q.K. Nguyen, R. Shanmugam, S. Sharma, T.T. Thuy Phan, H.G. Pham, H.T. Nguyen, Q.H. Nguyen, T.X. Nguyen, B. Pham, T.N. Mai Pham, R.R. Gangavarapu, Y.H. Su, J.M. Ting, D.T. Pham, *Adsorptive removal of oxytetracycline antibiotics on magnetic nanoparticles $NiFe_2O_4$/Au: Characteristics, mechanism and theoretical calculations*, Materials Chemistry and Physics, 323, 129672 (2024); https://doi.org/10.1016/j.matchemphys.2024.129672.
[14] I. Starko, T. Tatarchuk, Mu. Naushad et al. *Enhanced Activity of La-Substituted Nickel–Cobalt Ferrites in Congo Red Dye Removal and Hydrogen Peroxide Decomposition*, Water, Air, Soil, Pollution, 235, 527 (2024); https://doi.org/10.1007/s11270-024-07329-5.
[15] K.E. Kumar, A. Manikandan, V. Sathana, S. Muthulingam, M.M. Julie, R.T. Kumar, A. Dinesh, M. Durka, M.A. Almessiere, Y. Slimani, A. Baykal, A. Khan, *Impact of the rare earth elements doping on the copper ferrite spinel magnetic nanoparticles*, Elsevier Ltd, (2024); https://doi.org/10.1016/b978-0-323-85748-2.00014-1.
[16] T. Tatarchuk, I. Starko, *Mesoporous La-substituted nickel-cobalt ferrites synthesized via reduction method resulting in significantly enhanced adsorption properties*, Journal of Environmental Chemical Engineering, 13, 115657 (2025); https://doi.org/https://doi.org/10.1016/j.jece.2025.115657.
[17] P. Samoila, C. Cojocaru, I. Cretescu, C.D. Stan, V. Nica, L. Sacarescu, V. Harabagiu, *Nanosized spinel ferrites synthesized by sol-gel autocombustion for optimized removal of azo dye from aqueous solution*, Journal of Nanomaterials, 2015 (2015); https://doi.org/10.1155/2015/713802.
[18] J. López-Luna, L.E. Ramírez-Montes, S. Martinez-Vargas, A.I. Martínez, O.F. Mijangos-Ricardez, M. del C.A. González-Chávez, R. Carrillo-González, F.A. Solís-Domínguez, M. del C. Cuevas-Díaz, V. Vázquez-Hipólito, *Linear and nonlinear kinetic and isotherm adsorption models for arsenic removal by manganese ferrite nanoparticles*, SN Applied Sciences, 1, 1 (2019); https://doi.org/10.1007/s42452-019-0977-3.
[19] M.A. Islam, M.A. Chowdhury, M.S.I. Mozumder, M.T. Uddin, *Langmuir Adsorption Kinetics in Liquid Media: Interface Reaction Model*, ACS Omega, 6, 14481 (2021); https://doi.org/10.1021/acsomega.1c01449.

[20] U.A. Edet, A.O. Ifelebuegu. *Kinetics, Isotherms, and Thermodynamic Modeling of the Adsorption of Phosphates from Model*, Wastewater Using Recycled Brick Waste, Process, 8, 665 (2020); https://doi.org/10.3390/pr8060665.
[21] S.J. Olusegun, N.D.S. Mohallem, *Comparative adsorption mechanism of doxycycline and Congo red using synthesized kaolinite supported $CoFe_2O_4$ nanoparticles*, Environmental Pollution, 260, 114019 (2020); https://doi.org/10.1016/j.envpol.2020.114019.

Ірина Старко

Очищення забрудненої води феритовими наночастинками шпінелі, легованими La та Gd: кінетика та механізми адсорбції

Прикарпатський національний університет імені Василя Стефаника, Івано-Франківськ, Україна,
starkoiryna93@gmail.com

У роботі досліджено кінетику видалення барвника Конго червоного (КЧ) and антибіотика окситетрацикліну (ОТЦ) з водних розчинів синтезованими та відпаленими La- та Gd-вмісними наноферитами. Для оцінки механізму адсорбції були використані кінетичні моделі псевдо-першого порядку, псевдо-другого порядку, Еловіча та модель міжчастинкової дифузії. Показано, що адсорбція КЧ та ОТЦ на феритах найкраще відповідає кінетичній моделі псевдо-другого порядку. Рівновага адсорбції при видаленні КЧ та ОТЦ була досягнута через 60 хв для обох досліджуваних речовин. Відпал впливає на адсорбційні властивості зразків, збільшуючи початкову швидкість адсорбції відповідно до кінетичної моделі псевдо-другого порядку. Зокрема, початкова швидкість адсорбції КЧ на вже синтезованих і відпалених La- та Gd-вмісних феритах збільшується приблизно в 7 та 5 разів відповідно. Швидкість адсорбції ОТЦ також збільшилась у зразках після відпалу. Для зразка $Ni_{0.5}Co_{0.5}La_{0.02}Fe_{1.98}O_4$ швидкість покращилася в 1.8 раза. Для зразка $Ni_{0.5}Co_{0.5}Gd_{0.025}Fe_{1.975}O_4$ швидкість зросла в 3.6 раз. Проаналізовані дані показують, що молекули барвника та антибіотика адсорбуються на поверхні фериту шляхом хемосорбції.

Ключові слова: Ni-Co ферит; Лантан; Гадоліній; адсорбент; кінетична модель; шпінель; очищення води.